LOCATING EDGE POINTS IN BARHYMETRIC LIDAR DATA

Guo-Hao, Huang, Student
Chi-Kuei, Wang, Assistant Professor
Department of Geomatics National Cheng Kung University 1 University Road, Tainan, Taiwan, R.O.C. 701
p6894101@mail.ncku.edu.tw
chikuei@mail.ncku.edu.tw

KEYWORDS: bathymetric lidar; edge detection; point cloud

ABSTRACT: Airborne lidar (LIght Detection And Ranging) system has been proved cost effective for surveying near shore shallow water, where complicate and dangerous underwater environments prohibit the shipborne sonar survey. Such an area is usually of great importance for environmental management and natural resources inventory. Current algorithms for locating edge points assume the earth's surface is continuous in all directions and differ in how they measure discontinuities between surfaces from the bare earth. In this paper, the signal of the airborne bathymetric lidar system, which is affected by the reflectance of the bottom materials, is used to detect the change of the ocean bottom. We propose a procedure based on Kriging method and the difference of the kriging predicted value and original value to find edge points. A dataset of Egmont Key, FL, collected by SHOALS, is tested. Our results show that the procedure can produce consistent results of edge point locations.

1. INTRODUCTION

Airborne lidar system is widely used for automated generation of digital terrain models (DTM) and surface models (Ackermann, 1999). The lidar systems transmit laser pulses from an aircraft platform toward the bare earth and measure the return time to obtain corresponding ranges. The product of airborne lidar system is a dense cloud of 3D points. Bathymetric lidar systems are designed to measure the water depth in near shore water area, where sonar survey is too dangerous or too expensive to be conducted. Mapping of the near shore environment is important for environmental management and natural resources inventory. For example, locating bottom material is essential for fishery management (von Szalay and McConaughey, 2002).

Much work in airborne lidar systems have been done on automated filtering to classify the lidar points clouds into those that are part of the bare earth surface and those that are not. Some comparison of known filtering algorithms and difficulties have been mentioned in Sithole and Vosselman (2004). The lidar point clouds can be considered to be a representation of a piecewise continuous surface (the bare earth), whose continuity is broken by objects. As a result, the crucial part of filter algorithms is how to measure discontinuities between surfaces from the bare earth and surfaces from objects. The discontinuity includes height difference, slope, shortest distance to a parameterised surface and so on.

In this paper, we propose a procedure based on kriging method to find edge points of bathymetric lidar system and apply to the dataset of Egmont Key, FL, collected by Scanning Hygrographic Operational Airborne Lidar Survey (SHOALS) system. The preliminary results are promising for detecting ocean bottom change.

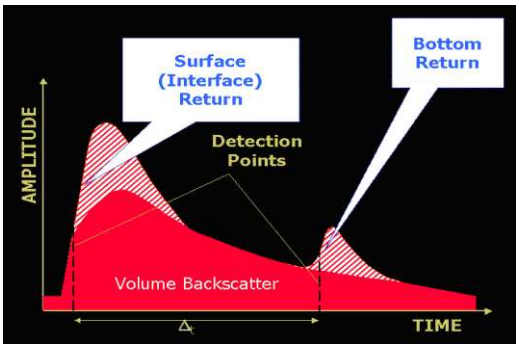

Figure 1: Generic received lidar signal (Guenther *et al.*, 2000).

2. METHOD

2.1 Concepts

The generic optical component of a bathymetric lidar system consists of a Nd-YAG laser source that can transmit pulsed laser of 6 ns at the wavelength of 1064 nm (infrared, fundamental frequency) and 532 nm (green, 2nd harmonic) and several receivers. The infrared laser pulse is used to detect the water surface; the green laser pulse is used to detect the ocean bottom. The generic received lidar waveform is shown in figure 1 (Guenther *et al.*, 2000).

From figure 2, the following observation can be made. Panel (a) of figure 2 shows an imaginary site consists of two bottom types, sand and coral, which do not change their reflectance with depth as seagrass. So one would expect to see two distinct curves representing the two bottoms. In the result of the difference curve shown in Panel (c) of figure 2, it is clear that at the boundary where the two bottoms meet, there is a double-peak feature, one positive and one negative. Thus the difference of the kriging predicted value and original value can be used to find edge points.

2.2 Theory

Kriging has been used to create smooth surface from point data because of its effectiveness of dealing with irregular data and because it provides the Best Linear Unbiased Estimate of the unsampled locations (Burrough and McDonnel, 1997). The estimated value is a linear combination of it neighbors with different weights. It can be written as:

$$\hat{Z} = \sum_{i=1}^{n} w_i Z(X_i)$$

$\hat{Z}$ is the value being estimated at location x; w_i are the weights; $Z(X_i)$ are the values at the neighboring locations. The weights can be obtained by $w_i = K^{-1}k$. K and k are the variance-covariance matrix between measured data points and between estimated and measured data points, respectively. The weights of ordinary kriging fulfill the condition: $\sum_{i=1}^{n} w_i = 1$. To obtain the variance-covariance matrix of k, one of the measures is to calculate the semi-variogram of the dataset and fit a theoretical variogram model to the result.

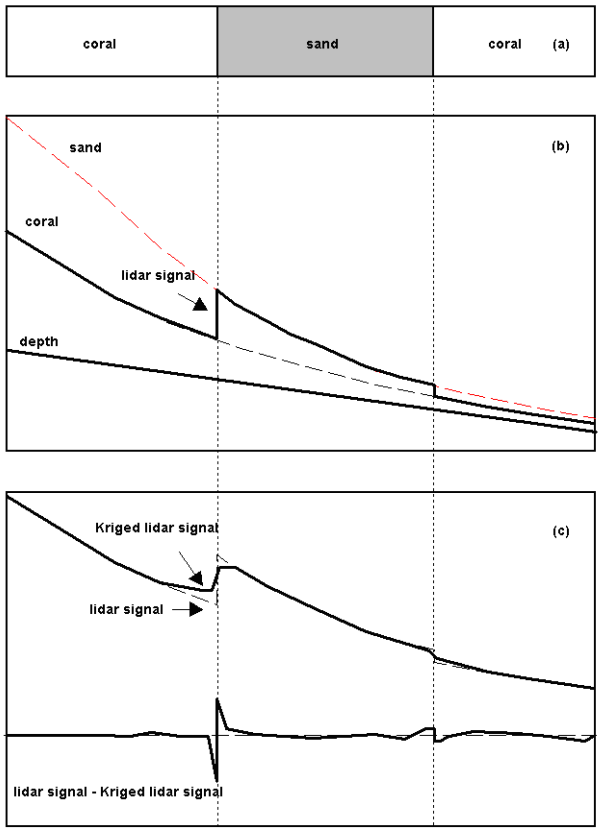

Figure 2: Using kriging technique to detect ocean bottom change. Panel (a) shows a imagenary site consist of two bottom types, sand and coral. Panel (b) shows the depth profile of this site, the therotical lidar signal of sand and coral at different depth, and the lidar signal of this imagernary site. Panel (c) shows the lidar signal after being smoothed by kriging, and the difference between the original lidar signal and the smoothed lidar siganal.

The semi-variogram can be presented as:

$$\gamma(h) = \frac{1}{2|N(h)|} \sum_{N(h)} (Z(x_i) - Z(x_j))^2$$

h is the distance between data pairs; $N(h)$ is the number of data points separated by distance h. Usually, a distance tolerance is associated with h to obtain sufficient data points in a certain lag. The semi-variogram summarizes the spatial relationships between data points within a particular dataset.

3. RESULTS

3.1 Data Sets

The lidar data for this research is provided by corps of engineers with their SHOALS system. The coverage includes the east coast of Egmont Key, Florida. These data was collected on May 15th, 2000 at the altitude of 400 m with sample spacing of 6 m by 8 m. In order to reduce the uncertainty of determining the water surface, the pulse light is fixed to enter the water with a nadir angle of 20 degree. Two datasets of adjacent flightlines are tested. The one that is near shore of 4045 data points is named side A; the other that is offshore of 7048 data points is named side B. The extents of two datasets overlaying on the NAPP (National Aerial

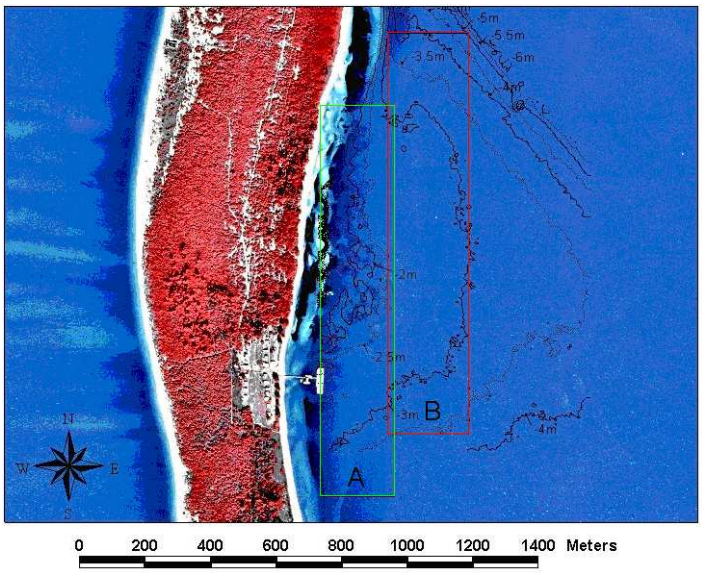

Figure 3: Egmont Key, FL: The green and red rectangles show side A and side B respectively.

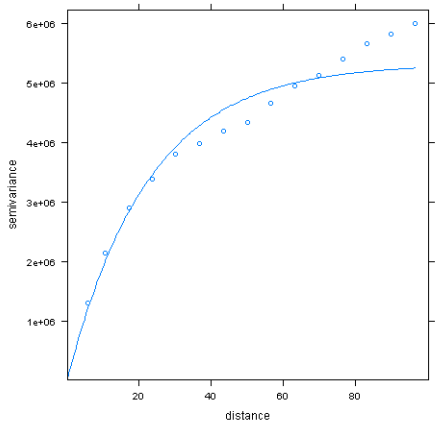

Figure 4: Exponential variogram model in data A

Photograph Program) photo in figure 3. In the paper, only the results of side A are listed.

3.2 Variogram Model

In the paper, we use software R to calculate variogram models. The lidar points are separated by 6 m $\sim$ 8 m and the purpose of kriging is to maximize the discontinuity discrepency. To minimize cpu and memory requirement and to obtain stable matrix operations, a search circle of 20 m is choosen for kriging. The result of fitted variogram models in side A is shown in figure 4. Figure 4 represents that exponential variogram model shows a better fit at 0 $\sim$ 20 m, hence is choosen.

3.3 Cross-validation

Based on the properties of the kriging operation, figure 5(a) and 5(d) show that the resultant cross-validation map is smoother than the original data. Because it is hard to draw conclusion from the resultant maps (figure 5(e)) of the difference between the kriging result and the original values, the contour maps are generated to guide the eye (figure 5(f)). Figure 5(b) is the result from the previously proposed procedure (Wang and Philpot, 2007). The threshold is

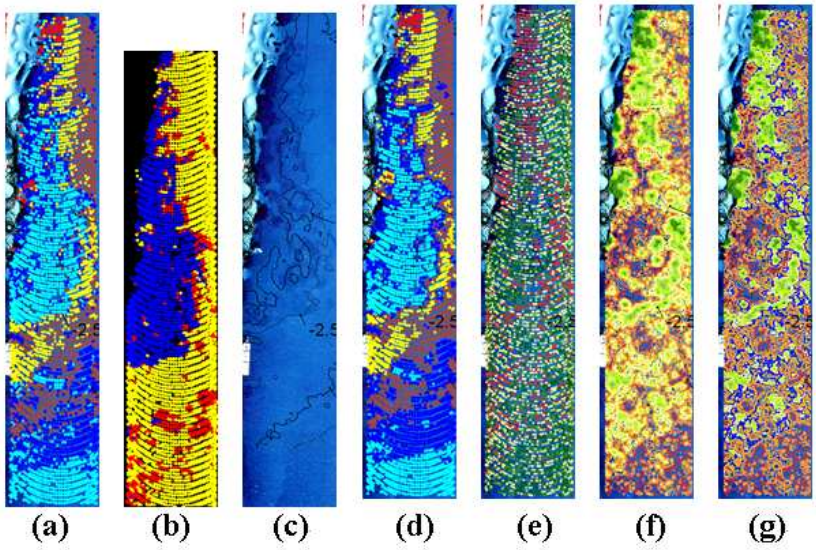

Figure 5: (a) The original lidar data of side A. (b) The result from the previously proposed procedure (Wang and Philpot, 2007). Blue is dark dense seagrass; red is bright patchy seagrass; yellow is sand. (c) The NAPP photo of the same area. (d) The kriging result of the original lidar data using a search circle with the radius of 20m. (e) The difference between (d) and (a). (f) The contour map of (e). (g) The contour map same as (f) with a threshold value shown blue.

chosen to match the result in figure 5(b). The contour map with the threshold can be seen in figure 5(g). Although the overall shape of seagrass edge is captured in figure 5(g), it doesn't form a continuous line.

In the consideration of removing the trend component, it is decided only to consider the understandable physical components. Hence, only depth is considered as the trend component, which increases with exponentially decreasing lidar data. Because of the high density of the data, which ensures an interpolation condition for every data point, the trend should not affect the result (Journel and Rossi, 1989). However, the data are still tested with its original values and the detrended values to make sure the conclusion drawn by Journel and Rossi (1989) is applicable to this data. The results are shown in figure 6. The contour maps of the residual lidar data (figure 6(g)) show a more continuous line delineating the edge of the dense seagrass, which suggest the results from the original data and the detrended data are different, and the results from the detrended data are better.

4. CONCLUSION

All of the kriging results shown in this paper are based on fitting variogram to the data range from 0 to 20 m in order to capture the local variation. It also shows that kriging method can be used to find edge points of bathymetric lidar systems. In addition, the kriging procedure can handle irregularly spaced data points. Divide and conquer strategy can be implemented, hence a large dataset will not be a problem. In the future, we will combine the kriging procedure and segmentation algorithms to find edge segments.

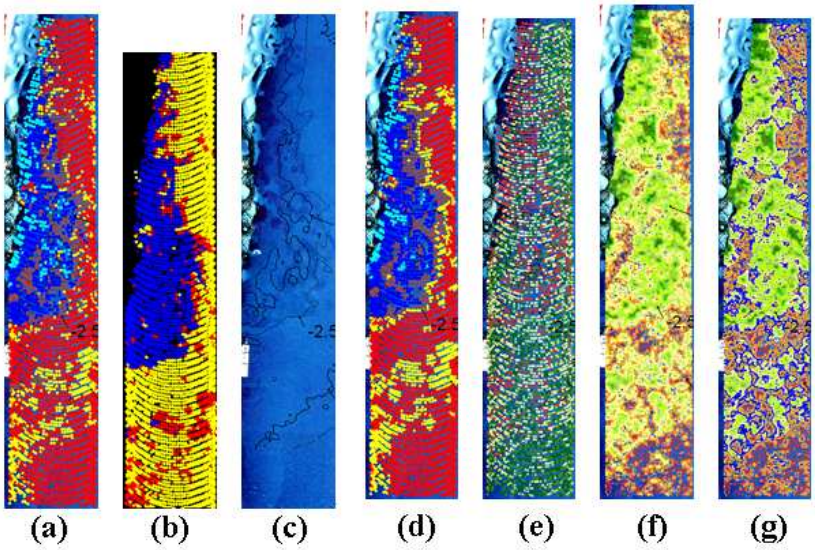

Figure 6: (a) The residual of the lidar data (detrended lidar data) of side A. (b) The result from the previously proposed procedure (Wang and Philpot, 2007). Blue is dark dense seagrass; red is bright patchy seagrass; yellow is sand. (c) The NAPP photo of the same area. (d) The kriging result of the residual lidar data using a search circle with the radius of 20m. (e) The difference between (d) and (a). (f) The contour map of (e). (g) The contour map same as (f) with a threshold value shown blue.

5. ACKNOWLEDGEMENT

The authors thank the support from National Science Council of Republic of China grant NSC 96-2628-E-006-084-MY3 and from National Cheng Kung University grant D96-3300 and D97-3300.

6. REFERENCES

Ackerman, F., 1999. Airborne laser scanning-present status and future expectations. ISPRS Journal of Photogrammetry & Remote Sensing. 54, pp. 64–67.

Burrough, P.A., and McDonnell, R.A., 1997. Principles of geographical information systems. Oxford University Press.

Guenther, G.C., Cunningham, A.G., LaRocque, P.E., and Reid, D.J., 2000. Meeting the accuracy challenge in airborne lidar bathymetry, presented at EARSel, Dresden.

Journel, A.G., and Rossi, M.E., 1989. When do we need a trend model in kriging, Mathematical Geology, 21, pp. 715–739.

Sithole G. and Vosselman G., 2004. Experimental comparison of filter algorithms for bare-earth extraction from airborne laser scanning point clouds. 54, pp. 85–101.

von Szalay, P.G. and McConnaughey, R.A., 2002. The effect of slope and vessel speed on the performance of a single beam acoustic seabed classification system. Fisheries Research, 54, pp. 181–194.

Wang, C.K., and Philpot, W.D., 2007. Using airborne bathymetric lidar to detect bottom type variation in shallow waters. Remote Sensing of Environment, 106, pp. 123–135.